

Optical and Structural Analysis of TiO₂ Nan Wires Deposited on Gallium Nitride Substrate and its Photo Detector Applications

^[1] Rosy Kimneithem Haokip, ^[2] Longjam Abungcha Meitei, ^[3] Pheiroijam Pooja, ^[4] Chitralkha Ngangbam, ^[5] Biraj Shougaijam

^{[1][2][3][4][5]} Department of Electronics and Communications, National Institute of Technology
Manipur, Imphal-795001, India

^[1] abungchameiteigate13@gmail.com, ^[2] rosy.kim@rediffmail.com, ^[3] pheiroipj93@gmail.com, ^[4] ng.chitra@gmail.com, ^[5] biraj.sh89@gmail.com

Abstract: Titanium Dioxide (TiO₂) Nanowires (NWs) were synthesized on p-GaN substrate using pressed and sintered TiO₂ material by Glancing Angle Deposition Technique (GLAD) inside the e-beam evaporation chamber. The XRD measurements indicates the presence of both rutile and anatase phase of TiO₂ crystals. The absorption measurement of p-GaN/TiO₂ NWs sample shows the absorption enhancement in Ultraviolet and visible region as compared to GaN (p)/TiO₂ Thin Film (TF) sample. The calculated band gap energy from the absorption measurement was found to be ~3.23eV. The photoluminescence (PL) measurement excitation at 340 nm shows the multiple peaks at ~3.3, ~3.1 and ~2.8 eV. The highest emission peak at ~3.3 eV from PL analysis may be the main band transition of TiO₂ NWs which also supports the band gap energy observed from absorption measurement. The fabricated Al/TiO₂ NW/TiO₂ TF/p-GaN based photodetector device gives a sharp rise time ~1.05 sec and fall time ~0.38 sec promising for optoelectronic applications.

Keywords: - Band gap, e-beam evaporation, GLAD, Photoluminescence, Titanium Dioxide (TiO₂)

I. INTRODUCTION

Ultraviolet (UV) photo detectors (PDs) have become widely popular in various applications such as space communication, ozone-layer monitoring and flame detection [1]. Recently, wide band gap metal semiconductors such as ZnO, TiO₂ have become very common in photo detector applications [2-6] due to its optical and electrical properties [7] such as high internal gain [2, 23]. Nanocrystalline TiO₂ has become very well known due to its potential for various applications such as photoconductors, environmental purifications, biomaterials, dielectric materials, generation of hydrogen gas [8,9], gas sensors, solar cells, light emitting diodes [10-12], and photo-catalysis [25,26]. TiO₂ crystals under UV radiation have high refractive index, high dielectric constant, high photosensitivity, and high optical transmittance in the visible as well the infrared region [13]. Due to its large band gap TiO₂ is photoactive under an excitation wavelength of less than 385nm which makes it useful in UV detection [12, 14]. It is a very powerful oxidant due to the oxidizing potential of the holes that are present in the valance band which are formed due to photo-excitation [10-11, 15]. TiO₂ nanowires (NWs) have become a potential application in optoelectronic devices due to its large surface-to-volume ratio producing large

photo-efficiencies [4, 22]. Photo detector based on perpendicular NWs minimizes the noise by restricting the collection of minority carrier charges at the electrode [24]. Tsung *et al.* reported the growth of 1-D TiO₂ NW based PDs by furnace oxidation of Ti/glass substrate. They produced high density single crystalline TiO₂ NWs [16]. However, fabrication of 1-D TiO₂ NWs on GaN substrate using pressed and sintered TiO₂ material could not be found in the literature. In this study, we report the fabrication of TiO₂ NWs from pressed and sintered TiO₂ material using Glancing Angle Deposition Technique (GLAD) inside the e-beam evaporator. Al nanoparticles (NPs) will be deposited on top of TiO₂ NWs as a metal contact. Structural property, optical as well as the electrical properties of the TiO₂ NWs will also be discussed.

II. EXPERIMENT

TiO₂ pellets are formed by compression of TiO₂ powder (99.999% pure (MTI, USA)) by using hydraulic press. The pellets are sintered at a temperature of 500° without reaching the melting point of TiO₂ material. This press and sintering process reduces the porosity and enhances the properties of the TiO₂ such as strength, electrical conductivity, translucency and thermal

conductivity. Before the growth of TiO₂ NWs, a p-type Gallium Nitride (GaN) substrate is cleaned subsequently with DI water for 30 seconds. TiO₂ NWs were synthesized from GLAD process on the TiO₂ thin film (TF) 30nm deposited on p-type GaN substrate. The substrates were placed inside the substrate holder which is kept at a perpendicular distance of 24 cm from the evaporation source. The substrates were subjected to a constant azimuthally rotation of 460rpm and the orientation of 85° with respect to the perpendicular line between the metal source and the substrate holder. The deposition rate of 1.2 Å/sec monitored by a quartz crystal was kept constant for the TiO₂ NWs and TiO₂ TF growth. Aluminum (Al) metal contact was made by evaporating it through an Al mask having a hole of diameter of 1.77 x 10⁻⁶ m². The crystal quality and the grain size of TiO₂ NWs were characterized by an X-ray Diffract meter (XRD, XPERT-PRO). A room temperature photoluminescence (PL) measurement was carried out at an excitation of 340nm using a Xenon lamp (ELICO, SL 174). The optical absorption measurement was performed on the samples using a UV-Vis near infrared spectrophotometer (Lambda 950, Perkin Elmer).

III. RESULTS AND DISCUSSION

A. XRD Analysis

Fig.1 shows the XRD diffraction pattern of the TiO₂ NWs on a p-type GaN substrate which indicates the presence of both the anatase and rutile phases respectively. The XRD pattern exhibits anatase peaks (101) and (200) observed at 2θ=5.83° and 48° respectively. It also exhibits rutile peak (111) observed at 2θ=43.75°. All the diffraction peaks agreed with the reported JCPDS card no. 21-1272 [17] for anatase peak at (101), JCPDS card no. 84-1286 [18] for anatase peak at (200) and JCPDS card no. 88-1175[18] for rutile peak at (111). The sample was found to be mostly crystalline in nature.

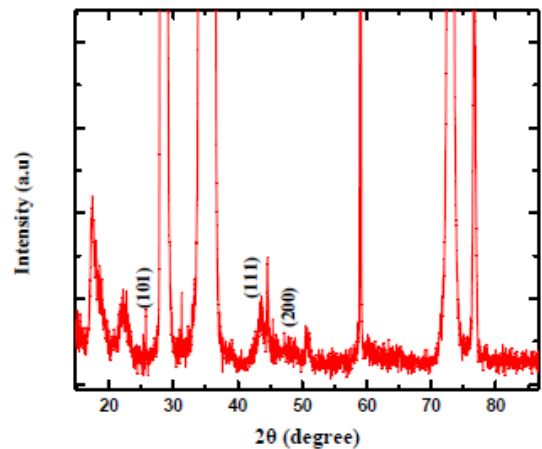


Fig.1 XRD analysis pattern of TiO₂ NW deposited on TiO₂

TF (50nm)/ p-GaN substrate. The grain size or the crystal size at the three peaks was calculated from Scherrer equation, $T = K\lambda/\beta\cos\theta$ (1) Where T= mean size of the crystalline domain which may be smaller or equal to the grain size, K is a dimensionless shape factor having a typical value of 0.9, λ= X-ray wavelength, β= Line broadening at half the maximum intensity (FWHM) = Δ (2θ), θ=Bragg's angle. Thus the TiO₂ NW crystals have an average grain size of ~1.30 nm which is anatase in nature. These crystals are responsible for the conductivity of the photo detector device.

B. Absorption Analysis

Fig. 2 (a) shows the optical absorption measurement was done on the TiO₂ TF and TiO₂NW/ TiO₂ TF samples, under the wavelength range of 315-700 nm at room temperature. The enhancement in absorption has been observed for TiO₂ NW /TiO₂ TF compared to TiO₂ TF in the UV-Visible region. It is observed that the absorbance intensity is maximum in the UV range of 315-400nm for the TiO₂ NW/ TiO₂ TF. It is also observed that the absorption is extended for the TiO₂ NW/ TiO₂ TF in the visible region of 400

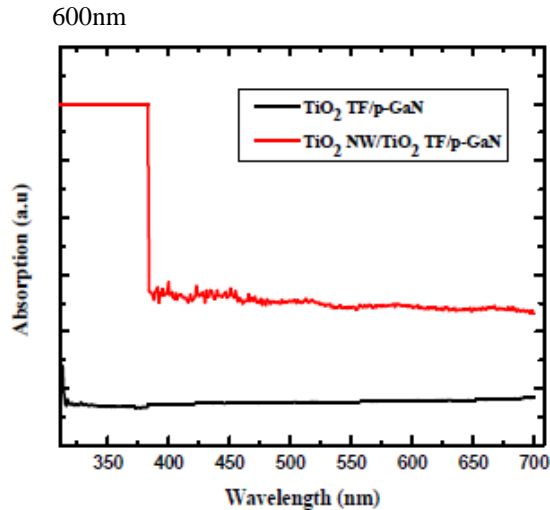


Fig. 2 (a) Absorption Spectra of TiO2 TF and TiO2 NW/TiO2

TF deposited on GaN substrate.

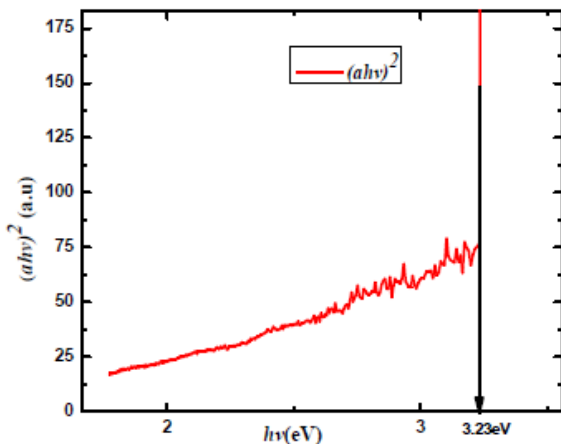


Fig. 2 (b) (ahv)2 versus photon energy (hv) for TiO2 NW/TiO2 TF

The absorption of TiO2 NW / TiO2 TF shows an enhancement of ~ 9 times in the UV region (315- 400 nm) and ~ 3.3 times in the visible region (400 - 600 nm) compared to the TF sample which was calculated. The fundamental absorption that corresponds to the transmission from the valance band to conduction band is taken into consideration to determine the band gap of the material. The direct band gap energy can be estimated from a plot of $(\alpha h\nu)^2$ versus photon energy $(h\nu)$ [19]. α is the absorption coefficient at each wavelength λ which is given by, $\alpha = 4\pi k/\lambda$ (2) and k = absorption index or absorbance.

By extrapolating the straight line portion of the $(\alpha h\nu)^2$ on the x-axis, the band gap is determined. The intercept of

the tangent to the plot gives a good approximation of the direct band gap energy of the sample. From Fig.2 (b) the direct band gap energy of the TiO2 NWs is found to be 3.23 eV.

C. Photoluminescence (PL) Analysis

Fig. 3 shows the PL spectrum of TiO2 NWs at an excitation wavelength of 340nm using a xenon lamp. Maximum peak is observed at the wavelength $\lambda=375.49$ nm. The optical band gap from PL is observed to be ~ 3.3eV. The optical band gap is calculated using the equation, $E_g = hc/\lambda = 1240.8/375.49 = 3.3$ eV

The smaller peaks at wavelengths 396.82 nm and 450.83 nm are due to the presence of defects in the TiO2 interstitials [20, 21]. The highest emission peak at ~3.3eV from PL analysis may be the main band transition of TiO2.NWs which is also near to the band gap energy observed from the measurement.

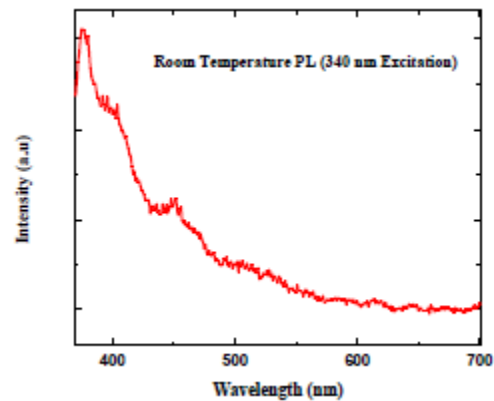


Fig. 3 Photoluminescence (PL) spectrum of TiO2 NW/TiO2 TF deposited on GaN substrate.

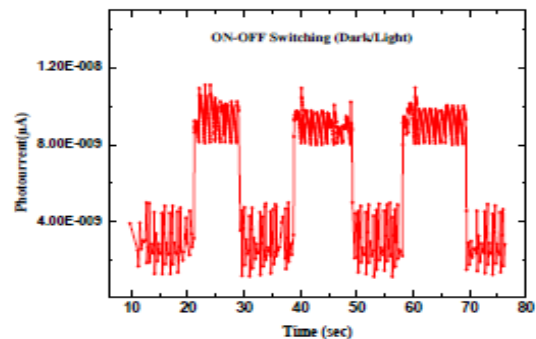


Fig. 4 Time response of the photo detector device under light illumination at +12 V.

D. Switching Characteristics

The switching characteristics of the TiO2 NWs based PD device was measured using Keithley Source

Meter (4200 SCS) and a white light source. Fig. 4 shows the time response of Al/TiO₂ NW/TiO₂ TF/p-GaN device at a biasing voltage of +12V on the top Al electrode. The light dependent current-time (I-T) characteristic of the device was measured under on/off switching of white light irradiation. Under light on, the photocurrent was increased from ~2.67nA to a maximum value of 11.1nA with a sharp rise time $\tau_r = 1.05$ secs and decay time $\tau_d = 0.38$ secs. The PD is showing very less decay time than the rise time. This indicates that the presence of defect states in the active TiO₂ NW region is very less [27, 28]. This decreases the diffusion of carriers into the active region thus making it a fast response light detector.

IV. CONCLUSION

In summary, we report the synthesis of pressed and sintered TiO₂ from TiO₂ powder and the fabrication of TiO₂ NWs on GaN substrate by GLAD technique. The polycrystalline structure of TiO₂ NWs is observed from XRD analysis. The optical absorption measurement gives the band gap energy ~3.23 eV. Also, the band gap energy from PL measurement is observed to be ~3.3eV. The smaller peaks at wavelengths 396.82 nm and 450.83 nm are due to the presence of defects in the TiO₂ interstitials. The photo detector device shows a fast response rise and fall time, promising for optoelectronic applications.

ACKNOWLEDGEMENT

The authors are grateful to the Microelectronics and Nan electronics (MAN) Lab and Chemistry Department, NIT Manipur for providing the facility for device fabrication, absorption and PL measurements. The authors are also grateful to Physics Department, Manipur University for technical support in getting the XRD analysis.

REFERENCES

[1] Tsung-Ying Tsai, Shoou-Jinn Chang, Sin-Hui Wang, Chiu-Jung Chiu, Cheng-Liang Hsu, and Ting- Jen Hsueh "TiO₂ nanowires UV Photodetectors with Ir Schottky Contacts," IEEE Photonics Technology Letters, Vol. 24, pp. 18, Sep 15, 2012.

[2] C. Soci, A.Zhang, B.Xiang, S.A Dayeh, D.P.R Aplin, J. Park, X.Y Bao, Y.H Lao, and D.Wang, "ZnO nanowire UV photo detectors with high internal gain," Nano Lett., Vol. 7, pp. 1003, 2007.

[3] G.Cheng, X.Wu, B.Liu, B.Li., X.Zhang and Z. Du, "ZnO nanowire Schottky barrier ultraviolet photodetector

with high sensitivity and fast recovery speed," Appl. Phys. Lett., Vol. 99, pp. 203105, 2011.

[4] P.Chinnamuthu, J.C Dhar, A. Mondal, A. Bhattacharya, and N.K Naik Singh, "Ultraviolet detection using TiO₂ nanowire array with Ag Schottky contact," J.Phys. D, Vol. 45, pp. 135102, 2012.

[5] L.Sang, M.Liao, and M. Sumiya, Sensors, "A Comprehensive Review of Semiconductor Ultraviolet Photodetectors: From Thin Film to One-Dimensional Nanostructures," Vol. 13, pp. 10482, 2013.

[6] F.Omnes, E. Monroy, E.Munoz, and J.L Reverchon, "Wide bandgap UV photodetectors: A short review of devices and applications," Proc. SPIE, Vol. 6473, pp. 64730E, 2007. 4

[7] P.Chinnamuthu, A.Mondal, J.C Dhar, and Naorem Khelchand Singh, "Visible light detection using Glancing Angle Deposited TiO₂ nanowire arrays," Japanese Journal of Applied Physics, Vol. 54, pp. 06FJ01, 2015.

[8] A. Mills, N. Elliot, G. Hill, D. Fallis, J.R Durrant, R.L Willis, "Preparation and characterization of novel thick sol-gel titania film photocatalysts," Photobiol, Sci, Vol. 2, pp. 591, 2003.

[9] L.Zhao, Y. Yu, L. Song, X. Hu, A. Larbot, "Synthesis and characterization of nanostructured titania film for photocatalysis," Appl. Surf Sci, Vol. 239, pp. 285, 2005.

[10] L. Castaneda, A. Maldonado and M. Olvera, "Sensing properties of chemically sprayed TiO₂ thin films using Ni, Ir, and Rh as catalysts," Sensors Actuate. B, Chem., Vol. 133,no. 2, pp. 687-693, 2008

[11] X. Wang and T.T Lian, "Solvothermal synthesis of C-N codoped TiO₂ and photocatalytic evaluation for bisphenol a degradation using a visible light irradiated LED photoreactor," Appl. Catal. B, Environ., Vol. 100, pp. 355-364, Aug., 2010.

[12] L.Shen *et al.*, "Performance improvement of TiO₂/P3HT solar cells using CuPc as a sensitizer," Appl. Phys. Lett., Vol. 92, no. 7, pp. 073307-1-073307-3, Aug., 2008.

[13] C.Ngangbam, B.Shougaijam, A.Mondal, "Dispersed Ag nanoparticles on TiO₂ nanowire clusters for photodetection," IEEE TENCON, Oct., 2014.

[14] W.Y Weng, T.J Hsueh, S.J Chang, S.J Chang, H.T Hsueh and G. J Huang, "A high responsivity GaN

nanowire photodetector,” IEEE J.Sel. Topics Quantum Electron., Vol. 17, no. 17, pp. 105-109, 2006.

[15] X. Hue *et al.*, “TiO₂ based metal-semiconductor-metal ultraviolet photodetectors,” Appl. Phys. Lett., Vol., 90, no. 20, pp. 530-532, Apr. 2011.

[16] Tsung-Ying Tsai, Shou-Jinn Chang, Wen-Yin Weng, Cheng-Liang Hsu, Sin-Hui Wang, Chiu-Jung Chiu, Ting-Jen Hsueh and Sheng-Po Chang, “A Visible-Blind TiO₂ nanowire photodetector,” Journal of the Electrochemical Society, Vol. 159, no. 4, pp. J132-J135, 2012.

[17] Thirugnanasambandan Theivasanthi and Marimuthu Alagar, “Titanium dioxide (TiO₂) Nanoparticles - XRD Analyses – An Insight”.

[18] Kheamrutai Thamaphat, Pichet Limsuwan and Boonlaer Ngotawornchai, “Phase Characterization of TiO₂ Powder by XRD and TEM,” Nat. Sci., Vol. 42, pp. 357 – 361, 2008.

[19] Ruby Chauhan, Ashavani Kumar, and Ram Pal Chaudhary, “Structural and optical characterization of Ag-doped TiO₂ nanoparticles prepared by a sol-gel method,” Res Chem Intermed, Vol. 38, pp. 1443-1453, 2012.

[20] I. Shalish, et al., “Grain-boundary-controlled transport in GaN layers,” Phys. Rev. B, vol. 61, no. 23, pp. 15573-15576, 2000.

[21] A.K. Srivastava, M. Deepa and S.Bhandari “Tunable nanostructures and crystal structure in titanium oxide films,” Nanoscale Res. Lett., Vol. 4, pp. 54-62, 2009.

[22] Z. Jin, L. Gao, Q. Zhou, and J. Wang, Sci. Rep., “High-performance flexible ultraviolet photoconductors based on solution-processed ultrathin ZnO/Au nanoparticle composite films,” Vol. 4, pp. 4268, 2014.

[23] J. Zou, Q. Zhang, K. Huang, and N. Marzari, Phys.Chem. C, “UltraViolet photodetectors based on Anodic TiO₂ Nanotube Array,” Vol. 114, pp. 10725, 2010.

[24] R. Graham and D. Yu, “Scanning photocurrent microscopy in semiconductor nanostructures,” Nano Lett., Vol. 12, pp. 4360 2012.

[25] A. Fujishima and K. Honda, “Electrochemical photolysis of water at a semiconductor electrode,” Nature, Vol. 238, pp. 37 1972.

[26] A. Fujishima, X. Zhang, and D. A. Tryk, “TiO₂ Photocatalysis and Related Surface Phenomena,” Surface Science Reports, Vol. 63, pp. 515, 2008.

[27] S. Chakrabartty, A.Mondal, M.B. Sarkar, B. Choudhuri, A.K. Saha, and A. Bhattacharyya, “TiO₂ Nanoparticles Arrays Ultraviolet- A detector with Au Schottky contact,” IEEE Photonics Technol, Lett., Vol. 26, pp. 1065, 2014.]

[28] J. Xing, H.Wei, E.J. Guo, and F.Yang, J. Phys. D, “Highly Sensitive fast-response UV photodetectors based